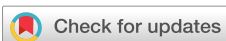


RESEARCH ARTICLE | FEBRUARY 28 2017

Side-group size effects on interfaces and glass formation in supported polymer thin films

Wenjie Xia  ; Jake Song; David D. Hsu; Sinan Keten



J. Chem. Phys., 146, 203311 (2017)
<https://doi.org/10.1063/1.4976702>

 CHORUS



Articles You May Be Interested In

Bulkier glass formability enhanced by minor alloying additions

Appl. Phys. Lett. (October 2005)

Effect of chemical structure on the isobaric and isochoric fragility in polychlorinated biphenyls

J. Chem. Phys. (April 2005)

Structure and dynamics of liquid methanol confined within functionalized silica nanopores

J. Chem. Phys. (October 2010)

Side-group size effects on interfaces and glass formation in supported polymer thin films

Wenjie Xia,^{1,a)} Jake Song,² David D. Hsu,³ and Sinan Keten^{1,3,b)}

¹Department of Civil and Environmental Engineering, Northwestern University, 2145 Sheridan Road, Evanston, Illinois 60208-3109, USA

²Department of Materials Science and Engineering, Northwestern University, 2145 Sheridan Road, Evanston, Illinois 60208-3109, USA

³Department of Mechanical Engineering, Northwestern University, 2145 Sheridan Road, Evanston, Illinois 60208-3109, USA

(Received 5 December 2016; accepted 30 January 2017; published online 28 February 2017)

Recent studies on glass-forming polymers near interfaces have emphasized the importance of molecular features such as chain stiffness, side-groups, molecular packing, and associated changes in fragility as key factors that govern the magnitude of T_g changes with respect to the bulk in polymer thin films. However, how such molecular features are coupled with substrate and free surface effects on T_g in thin films remains to be fully understood. Here, we employ a chemically specific coarse-grained polymer model for methacrylates to investigate the role of side-group volume on glass formation in bulk polymers and supported thin films. Our results show that bulkier side-groups lead to higher bulk T_g and fragility and are associated with a pronounced free surface effect on overall T_g depression. By probing local T_g within the films, however, we find that the polymers with bulkier side-groups experience a reduced confinement-induced increase in local T_g near a strongly interacting substrate. Further analyses indicate that this is due to the packing frustration of chains near the substrate interface, which lowers the attractive interactions with the substrate and thus lessens the surface-induced reduction in segmental mobility. Our results reveal that the size of the polymer side-group may be a design element that controls the confinement effects induced by the free surface and substrates in supported polymer thin films. Our analyses provide new insights into the factors governing polymer dynamics in bulk and confined environments. Published by AIP Publishing. [<http://dx.doi.org/10.1063/1.4976702>]

I. INTRODUCTION

It is widely appreciated that interfaces with substrates and free surfaces can significantly affect the dynamics and mechanical properties of polymers under confinement at nanoscale, which is important for applications such as nanoelectronics,¹ nanocomposites,² and biomedical devices.³ Nanostructured polymer systems can exhibit dramatic shifts in glass formation dynamics compared to the bulk state, which is commonly quantified by changes in their glass transition temperature, T_g .^{4–10} For freely standing or supported films that weakly interact with a substrate, the dynamics of polymers are enhanced due to a mobile “liquid-like” layer formed near the free surface, which generally causes a reduction in T_g .^{4,6,8,11–13} On the other hand, for polymers confined by a strongly attractive substrate, their dynamics are generally suppressed, leading to an increase in T_g .^{14–17} For polymer films with the presence of both free surface and substrate-film interface—a common setup for many polymeric nano-devices—their effects often compete, causing a change in T_g that depends not only on the film thickness but

also on many other factors, such as adhesive interactions and existence of an additional underlayer.^{14,18–22} Despite progress, there is still a lack of fundamental understanding of how molecular characteristics arising from monomer structure influence the glass transition of polymer thin films.

To understand the molecular mechanisms behind the glass formation of confined polymers, it is important to understand their properties in bulk. Recent studies have already proved that molecular features and characteristics are indeed important in determining bulk glass formation dynamics. For instance, there has been growing evidence suggesting that the fragility of glass formation is strongly associated with molecular features, such as chain stiffness and architecture.^{23,24} That is, polymers with higher chain stiffness that cause more packing frustration generally exhibit higher bulk fragility and T_g . These findings are consistent with the predictions of molecular simulations and theories, such as the general entropy theory (GET) of glass formation^{25,26} and the elastically collective nonlinear Langevin equation (ECNLE) theory.^{27,28} If fragility is considered to be a manifestation of the molecular structure of a polymer, an important question to address is how the fragility and molecular structure relate to T_g -confinement phenomena in nanoscale polymer films.

Several studies have aimed to draw a connection between this molecular picture and the free surface confinement effects on the glass transition of polymer thin films. For example,

^{a)}Present address: Materials Science and Engineering Division, National Institute of Standards and Technology, 100 Bureau Drive, M/S 8550, Gaithersburg, MD 20899-8550, USA.

^{b)}Author to whom correspondence should be addressed. Electronic mail: s-keten@northwestern.edu. Tel.: 847-491-5282.

many investigations have suggested that polymers with greater fragility exhibit a larger decrease in T_g in thin films.^{12,29,30} Assuming that the effect of free surface is dominant over the substrate, Torkelson and co-workers have argued that the extent to which the free surface relieves the packing frustration experienced by polymer chains near the surface can be correlated to the polymer's fragility in the bulk.¹² However, the relationship does not appear to hold in other polymer systems. Contrasting observations have been made both experimentally³¹ and computationally,³² where polymers with increased backbone stiffness (and thus larger fragility) exhibit reduced free surface confinement effects on film T_g reduction.

The molecular picture of confinement phenomena is even more lacking for systems under the influence of a strongly attractive substrate. Previous studies have made strides in identifying the effect of substrate features, such as substrate roughness and interfacial interaction strengths, on the overall T_g shift of the supported film.^{14,21,33–35} However, an in-depth investigation of the effect of molecular characteristics on the effect of the attractive substrate remains to be explored. If the correlation between molecular structure and the free-surface induced confinement effect is assumed to be valid, we can hypothesize that molecular structure should play an important role in determining the T_g changes near the substrate-film interface. The present work aims to investigate this possibility computationally.

Relating molecular features such as monomer structure to glass formation processes in a supported polymer film requires us to separate the free surface and substrate effects in thin films. Here, we use coarse-grained (CG) molecular dynamics (MD) simulations to quantify how side-group size (i.e., volume or bulkiness) plays a role on the T_g -confinement effects in supported polymer thin films. We employ our recently developed two-bead-per-monomer (one backbone bead and one side-group bead) CG model of poly(methyl methacrylate) (PMMA), which has been parameterized from all-atomistic (AA) simulations to match the dynamic and mechanical properties and density.³⁶ To understand the role of side-group size in glass transition of polymer films, we generalize our model and systematically change the van der Waals radius of the side-group CG bead by varying the Lennard-Jones (LJ) parameter σ . Our study starts from an investigation of bulk glass formation properties, and then we systematically explore how the side-group size affects the T_g -confinement phenomena in polymer thin films supported by the substrate. Our simulations reveal that the side-group size has a prominent effect on the interfacial confinement behaviors of supported polymer thin films through its influence on interfacial packing, wetting, and relaxation.

II. SIMULATION METHODS

We adopt an atomistically informed 2-bead type CG model of PMMA, where the backbone bead “A” incorporates the methacrylate group ($C_4O_2H_5$) and the side-group bead “B” includes the methyl group (CH_3) (Fig. 1(a)). The CG model was originally developed for simulating methacrylate-based polymers spanning both small and bulky side-groups, employing a universal backbone chain structure but a distinct

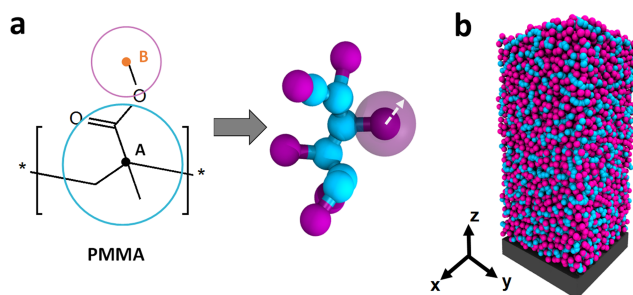


FIG. 1. (a) Schematic of the generalized two-bead CG model with varying side-group bead size σ_{BB} (marked by the arrow) based on the original CG model of PMMA. (b) Snapshot of the supported thin film model.

side-group. Here, to study the effect of side-group volume, we simply focus on changing the side-group van der Waals radius. As discussed extensively in the original paper,³⁶ the CG bonded interactions, including bonds, angles, and dihedrals, are derived by matching the all-atomistic (AA) bonded probability distributions using the Inverse Boltzmann method (IBM).^{37,38} Notably, the non-bonded interactions are captured by the Lennard-Jones (LJ) interactions

$$U_{\text{nonbond}}(r) = 4\epsilon \left[\left(\frac{\sigma}{r} \right)^{12} - \left(\frac{\sigma}{r} \right)^6 \right] \quad r < r_{\text{cut}}, \quad (1)$$

where σ is the effective van der Waals radius of the CG model at which U_{nonbond} is zero and ϵ is the depth of the potential well in energy unit. The cutoff distance r_{cut} is set to be 15 Å. The LJ parameters are tuned to match the density and T_g of the AA bulk systems.

For the 2-bead CG model, there are six different parameters for U_{nonbond} : σ_{AA} and ϵ_{AA} for backbone and backbone (AA) interactions, σ_{BB} and ϵ_{BB} for side-group and side-group (BB) interactions, and σ_{AB} and ϵ_{AB} for backbone and side-group (AB) interactions. The cross-interaction terms σ_{AB} and ϵ_{AB} are taken as the arithmetic ($\sigma_{AB} = \frac{1}{2}(\sigma_{AA} + \sigma_{BB})$) and geometric averages ($\epsilon_{AB} = \sqrt{\epsilon_{AA}\epsilon_{BB}}$) of the AA and BB terms, respectively. To generalize our model for the investigation of how the side-group size influences the glass transition of polymer systems, we systematically vary the side-group size by having σ_{BB} take the values 3.42 Å, 4.42 Å (original CG PMMA value), 5.00 Å, and 5.42 Å as illustrated in Figure 1(a). We keep σ_{AA} as a constant value of 5.5 Å. These polymer systems are denoted as s1, s2, s3, and s4, respectively. Functional forms of the potentials utilized by the CG models can be found in Table S1 in the [supplementary material](#).

All CG-MD simulations in this work are carried out using the LAMMPS package.³⁹ To simulate a bulk system, periodic boundary conditions are applied in all three dimensions. Each system consists of $N = 20\,000$ CG atoms with a chain length of $n = 200$. Using an integration time step of $\Delta t = 4$ fs, an energy minimization is performed using the conjugate gradient algorithm,⁴⁰ followed by annealing cycles with the NPT ensemble by cycling the temperature from 210 K to 750 K over a period of 4 ns until the density and energy of the systems have been fully equilibrated. Supported thin film systems are simulated with a thickness of ~18 nm in the z dimension and 9 nm in the x and y dimensions (Fig. 1(b)). Periodic boundary conditions are applied to the x and y dimensions, while the z dimension is

kept non-periodic in order to simulate a free surface on the top of the film. An implicit energetic wall is placed at the bottom of the film to represent the substrate. This substrate interacts with the polymer via a LJ 12-6 potential of the form

$$U_{\text{sub}}(z) = 4\varepsilon_{\text{sp}} \left[\left(\frac{\sigma_{\text{sub}}}{z} \right)^{12} - \left(\frac{\sigma_{\text{sub}}}{z} \right)^6 \right] \quad z < z_{\text{cut}}, \quad (2)$$

where z denotes the distance between the substrate and the polymer CG atoms, ε_{sp} denotes the adhesive interaction strength, $\sigma_{\text{sub}} = 4.5 \text{ \AA}$ denotes the polymer-substrate distance at which the potential crosses zero, and $z_{\text{cut}} = 15 \text{ \AA}$ is the cutoff interaction distance between the film and substrate. In order to observe a clear substrate effect, we choose a value of $\varepsilon_{\text{sp}} = 3 \text{ kcal/mol}$, which is comparable with the nonbonded cohesive interaction strength ε , leading to an adhesion energy of $\sim 100 \text{ mJ/m}^2$ that is achievable experimentally for atomically smooth surfaces. All the simulations of films are performed under the canonical ensemble (NVT). It should be noted that although the NVT ensemble is adopted for thin film simulations, the presence of free surfaces effectively leads to an isothermal-isobaric ensemble (NPT).

Structural relaxation dynamics of both the bulk and film systems is quantified by calculating the self-part of the intermediate scattering function

$$F_s(q, t) = \frac{1}{N} \sum_j^N \langle \exp[-iq \cdot (\mathbf{r}_j(t) - \mathbf{r}_j(0))] \rangle, \quad (3)$$

where N is the total number of beads, $q = |\mathbf{q}|$ is a wave number taken from the initial peak of the static structure factor $S(q)$, $\mathbf{r}_j(t)$ is the position of the j th particle at time t , and $\langle \dots \rangle$ is the ensemble average. Although our previous study has identified the q value for calculating $F_s(q, t)$ of the CG model of PMMA,⁴¹ this value will not necessarily be the same if we change the chemical structure of the CG model by changing σ_{BB} . Accordingly, we calculate the static structure factor $S(q)$ for bulk systems of different σ_{BB} and identify q based on the location of the first peak of $S(q)$. $F_s(q, t)$ is then evaluated with the identified q value and then fitted using the Kohlrausch-Williams-Watts (KWW) stretched exponential function of the form: $F_s(q, t) = C \exp[-(\frac{t}{\tau_{\text{KWW}}})^\beta]$, where C and τ_{KWW} are the fitting parameters and β is the “stretching exponent.” Consistent with many prior simulation works, we define the segmental relaxation time τ_α as the time at which $F_s(q, t) = 0.2$.^{20,41,42} It should be noted that $F_s(q, t)$ is different from that of a full intermediate scattering function, which yields slightly different values of τ_α . However, it has been shown in many prior

studies that the trend of glass formation by using the two functions is generally very consistent. The temperature dependent τ_α results are fitted using the Vogel-Fulcher-Tamman (VFT) function^{43–45}

$$\tau_\alpha = \tau_0 \exp \left(\frac{DT_0}{T - T_0} \right), \quad (4)$$

where τ_0 , T_0 , and D are treated as the fitting parameters associated with glass formation: T_0 is the end-of-glass formation temperature (also known as the Vogel-Fulcher temperature) and D describes the strength of temperature dependence of τ_α and is inversely related to fragility. To quantify glass transition, we use the commonly employed “computational T_g ” as defined by the temperature at which τ_α reaches 1 ns, when the systems have begun to fall out of equilibrium.^{24,41,42,46}

III. RESULTS AND DISCUSSION

Prior to studying the confinement behaviors of thin film systems, we first investigate how the local structural and glass formation properties of bulk systems change with increasing the “bulkiness” of the side-group (i.e., increasing σ_{BB}). To characterize the local molecular structure in the bulk state, we calculate the static structure factor $S(q)$, which provides information on the mean correlations in the positions of segments in the polymer. Fig. 2(a) shows the results of $S(q)$ for different σ_{BB} at $T = 350 \text{ K}$. It can be observed that the location of the first major peak of $S(q)$ decreases with increasing σ_{BB} , indicating a less dense packing as the side-group size becomes larger. This can also be observed from the radial distribution function $g(r)$ as shown in Fig. 2(b), where the first peak in $g(r)$ is located at a greater radial distance r for larger side-group size. These results are reasonable, as decreasing σ_{BB} should reduce the excluded volume created by the side-group, making other chains pack more densely. The wave number q at the location of the first peak of $S(q)$, which is listed in Table I, is then used for calculating the segmental relaxation via $F_s(q, t)$ for different CG systems.

Using the segmental relaxation data, we characterize the bulk relaxation, T_g , and fragility (defined by $K = 1/D$)⁴⁷ of our model systems. As shown in the τ_α data in Fig. 3(a), CG polymer systems with larger side-groups require longer times to relax at a given temperature. This is manifested by the systems with larger side-groups experiencing lower D (Fig. 3(b)) and larger T_g (Fig. 3(c)). The values of K and T_g are also summarized in Table I. Our finding on the side-group size effect on the glass formation is qualitatively consistent with the GET

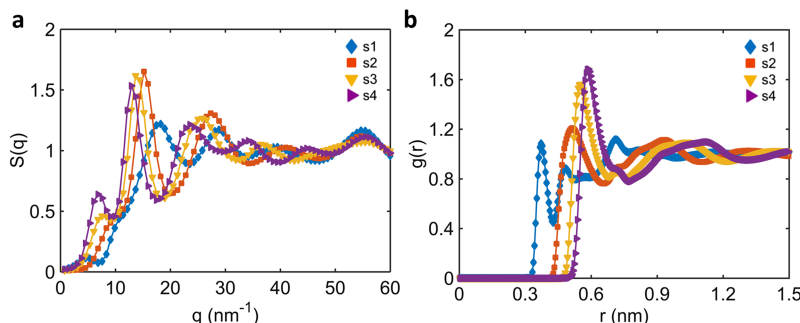


FIG. 2. (a) Structure factor $S(q)$ and (b) radial distribution function $g(r)$ for CG bulk systems with different side-group sizes at $T = 350 \text{ K}$.

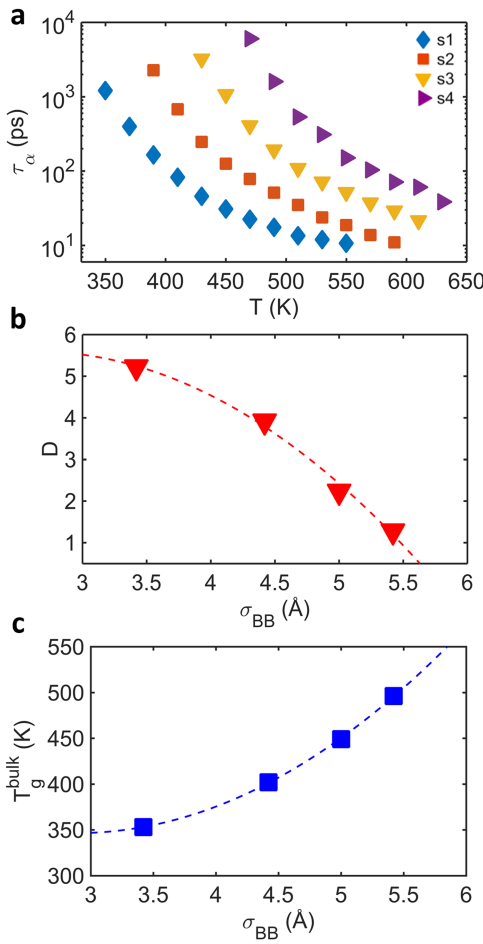


FIG. 3. (a) Segmental relaxation time τ_α as a function of temperature for different bulk systems. Influence of side-group bead size (σ_{BB}) on the bulk glass-forming properties (b) D and (c) T_g^{bulk} . The dashed lines in the plots show the trend.

predictions for the relative flexible backbone and stiff side-group (F-S) class of polymers.⁴⁷ It should be noted that a similar side-group size effect on glass formation is observed by applying the same q as that in s1 for all four systems (Fig. S1 in the supplementary material).

Our findings indicate that the side-group size has a similar effect to increasing the polymer's stiffness (i.e., either the backbone^{25,26,32} or the side-chain stiffness^{11,26,30}) with regards to increase in fragility. However, the mechanism of the side-group size effect on molecular packing and fragility may not be the same as that of the stiffness effect. Prior studies have shown that the observation of fragility based on stiffness is nonmonotonically dependent on the ratio of backbone and side-group stiffnesses,^{23,26} suggesting a fundamental

TABLE I. Comparison of structural and glass formation properties of the different CG bulk systems.

System	σ_{BB} (Å)	q (nm ⁻¹)	$K (= \frac{1}{D})$	T_g (K)
s1	3.42	17.47	0.19	352
s2	4.42	15.19	0.26	402
s3	5.00	13.67	0.45	449
s4	5.42	12.91	0.78	496

difference between side-group size and stiffness effects on glass formation properties. Moreover, previous studies on antiplasticizers⁴⁸ and diluents²⁴ have both suggested that the inclusion of small molecules or spheres assists in polymer packing behavior and lower bulk fragilities, which support our findings that side-group bulkiness is an important factor in glass formation behavior.

Next, we proceed to examine the confinement behaviors of the supported thin film systems using the CG models. Fig. 4(a) shows the representative τ_α vs. T results, along with the VFT fits (solid and dashed curves) for all the different systems in the bulk and thin film states. It can be observed that all the systems exhibit faster relaxation in the film compared to bulk. As the side-group size increases, the shift in relaxation dynamics between bulk and film becomes more pronounced. As shown in Fig. 4(b), the confinement effects are observed in all the film systems as indicated by a negative value of $\Delta T_g (= T_g^{\text{film}} - T_g^{\text{bulk}})$, which implies that the free-surface effect plays a dominant role in the film confinement behaviors. From our result, it is evident that these confinement effects on film T_g are apparently enhanced for polymers with larger side-group size and higher fragility. Our findings are consistent with recent experimental observations by Torkelson *et al.*, who have shown a one-to-one correlation between fragility and the strength of confinement effect in silicon supported thin films without substantial interactions with the substrate,^{12,49} as well as computational results by Xie *et al.*,³⁰ who have investigated the effects of side-chain stiffnesses on ΔT_g . However, they do not agree with the results of Shavit *et al.*³² and Torres *et al.*,³¹ who investigated polymers with stiffer backbones and found no such correlation between fragility and ΔT_g . One possible reason for the discrepancy between these findings may

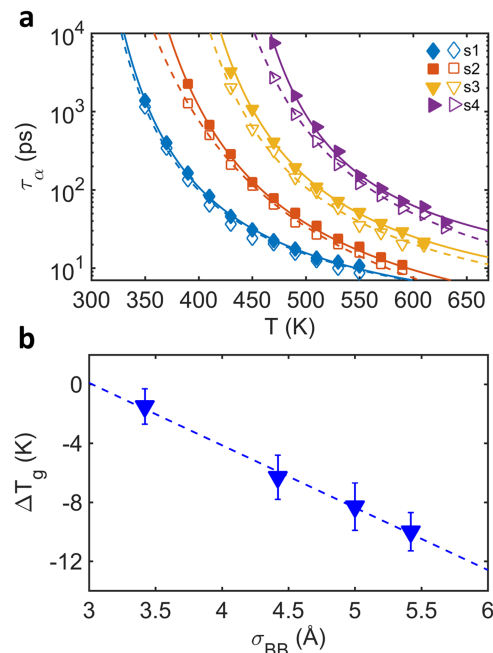


FIG. 4. (a) Comparison of temperature dependent relaxation time τ_α between the bulk (filled symbols) and supported film systems (open symbols). The solid and dashed lines show the VFT fits for the bulk and film systems, respectively. (b) Dependence of T_g depression of the film on side-group size σ_{BB} . Dashed line illustrates the trend.

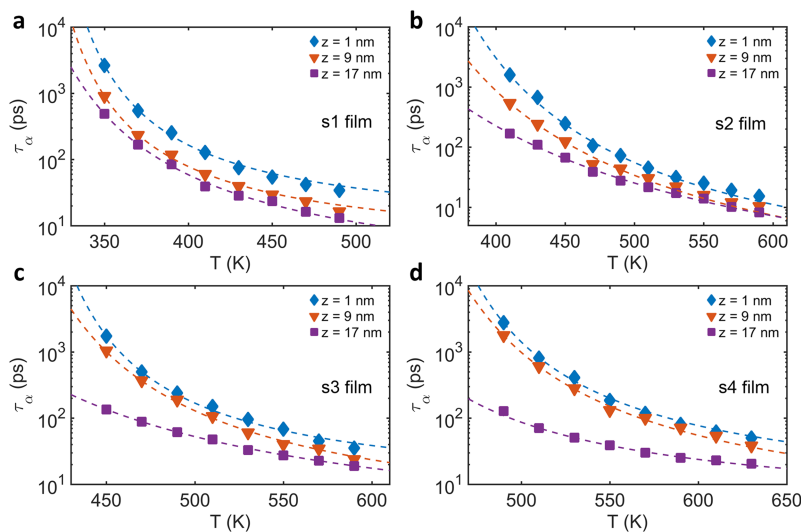


FIG. 5. Local relaxation time τ_α near the substrate-film interface ($z = 1$ nm), in the middle ($z = 9$ nm), and near the free surface ($z = 17$ nm) for the (a) s1, (b) s2, (c) s3, and (d) s4 film systems. The dashed lines show the VFT fits.

be the chain ordering and alignment effect induced by the rigid backbone of the polymers near the free surface.³² Therefore, it is believed that there are other factors that may cause the contrast observations on T_g -confinement behaviors and their correlation with polymer fragility.

So far, our result indicates that a larger side-group can reduce packing efficiency, which contributes to an altered confinement effect due to a free surface. However, how the strength of the confinement effect in an attractively supported polymer film depends on the side-group size and polymer fragility remains unclear based on our current results and available experimental data. We can, however, hypothesize that the bulkiness of the side-group and its impact on fragility should play a role in determining the T_g perturbations near the substrate-film interface.

Local relaxation dynamics and spatial T_g distribution within the films should provide deeper insights into the confinement effects by allowing us to partition the relative roles of the free surface and the substrate in influencing the glass transition of the films. As such, we quantify T_g locally in the film by quantifying relaxation as a function of monomer position z in the film, as measured from the substrate-film interface to the free surface. The thickness of the layer to quantify τ_α in the local region is 2 nm. Fig. 5 shows the results of the representative local τ_α vs. temperature for the different film systems. For all the systems, we can observe that the temperature dependent $\tau_\alpha(z)$ decreases as the film position shifts from the region near the substrate interface ($z = 1$ nm) to the bulk-like center region ($z = 9$ nm) and the free surface region ($z = 17$ nm), which indicates local T_g variation within the films. Another important observation is that the shift in local τ_α as marked by the VFT curves is qualitatively different as the side-group size increases. The shift of the local τ_α from the substrate interface region to the middle region is much larger as the side-group size increases from s1 to s4. However, as the position moves from the middle to the free surface region, the trend seems to reverse—the shift of the local τ_α is less for the system with smaller side-group size. These results imply that the strength of the confinement effects is distinct for films with different side-group sizes.

Fig. 6 shows the result of the local T_g normalized by bulk T_g in the supported film for different systems. There exists a clear local T_g gradient with the magnitude decreasing from the substrate-film interface to the free surface. Although the overall film T_g is lower than that of the bulk, the local T_g of a polymer in the region near the substrate ($z < \sim 5$ nm) is enhanced compared to the bulk. This can be attributed to the attractive interactions between the polymer and the substrate, which slows down chain relaxation and dynamics near the substrate. In the interior region (~ 5 nm $< z < \sim 10$ nm), the T_g becomes close to the bulk values, indicating a bulk-like response within the film. Towards the free surface ($z > \sim 10$ nm), the T_g becomes appreciably lower than the bulk value due to the enhanced mobility near the surface as also observed for ΔT_g . The observation of the local T_g variation within the supported films is in line with the general picture of a commonly employed tri-layer model:^{5,50} a substrate-interface layer, an interior bulk-like layer, and a free-surface layer, which are useful to describe the confinement behaviors of the supported films as illustrated in the inset of Fig. 6.

Comparing the local T_g results for different film systems, we see a more obvious correlation between σ_{BB} and

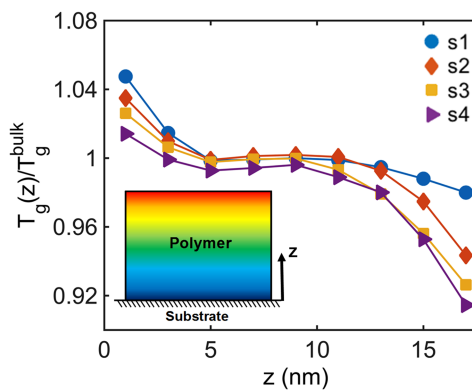


FIG. 6. Local T_g normalized by T_g^{bulk} as a function of the film position z from the substrate-film interface to the free surface. The inset illustrates the local T_g gradient within the film.

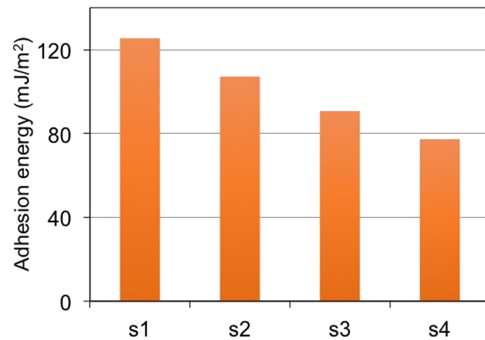


FIG. 7. Dependence of the substrate–film adhesive energy on the side-group size. Increasing the side-group size decreases the adhesion energy as less chains can be packed onto the interfacial layer.

confinement effect on the local T_g in the films. As the side-group becomes larger, the magnitude of local T_g reduction near the free surface is greater, which indicates a stronger free-surface effect and is consistent with prior studies and the fragility hypothesis. Interestingly, however, we see a reduced T_g -confinement effect near the substrate for a larger side-group size. This result suggests that there exists a correlation between the fragility and the strength of confinement effect induced by the substrate, which contrasts what is observed near the free surface. This effect may be partially attributed to the fact that polymer chain packing on and near the surface is greatly hindered for larger side-groups, which lowers the effective adhesion energy between the surface and the polymer film.⁵¹

The result shown in Fig. 7 seems to support this, as it shows a decrease in adhesion energy with increasing the side-group size. Lower adhesion energy will lead to a lower substrate-induced appreciation of local T_g . This finding is also consistent with experimental observations. For methacrylate polymers, strong interfacial interaction between silica substrates and films is achieved via hydrogen bonding formed by the polar groups (e.g., ester and hydroxyl groups) in polymer chains. For larger side-group sizes, the packing efficiency and the density of polymer chains near the interface are lower. Larger side-groups can reduce the hydrogen-bond density near

the interface and lead to lower adhesion energy, which is similar to our observation from simulations. The side-group size effect on adhesion energy is also evidenced in a previous work by Priestley *et al.*¹⁵ They observed that the enhancement in local T_g near the silica substrate is greater for PMMA with a smaller side-group than poly(ethyl methacrylate) (PEMA) with a relatively larger side-group, which could be attributed to the difference in local molecular packing and adhesion energy. Overall, this analysis also reveals why ΔT_g becomes more substantial with increasing σ_{BB} , as observed in Fig. 4(b), as it shows that the drop in adhesion energy and the rising influence of the free surface tilt the balance of the competition in favor of the free-surface effect on T_g .

We further probe the polymer packing efficiency near the substrate by evaluating the Debye-Waller factor (DWF) in different regions of the film. Recent studies have suggested a fundamental role of the DWF in predicting the glass formation dynamics and stiffness of polymers in the bulk and confined states.^{34,52–54} The DWF is a dynamic measurement of the segmental “free volume” explored by the chain segments on the order of picosecond time scale.⁵⁵ This property can also be experimentally measured via incoherent neutron scattering (INS) experiments.^{53,56} The DWF also provides information on local molecular stiffness associated with the caging effect of neighboring atoms.^{54,57–59} To gain insights into the confinement effect on local dynamics and packing, we analyze the local DWF $\langle u^2 \rangle$ across the supported films. In our simulations, we define $\langle u^2 \rangle$ as the value of the local mean-squared displacement (MSD) g_0 at $t = 4$ ps, which is calculated as

$$g_0(t, z) = \left\langle \frac{\sum_{i=1}^N \delta[z - z_i(0)][r_i(t) - r_i(0)]^2}{\sum_{i=1}^N \delta[z - z_i(0)]} \right\rangle, \quad (5)$$

where $r_i(t)$ is the position of the i th CG bead at time t , δ is the Dirac delta function, and $\langle \dots \rangle$ denotes the ensemble average. The CG atoms are sorted into each bin with a thickness of 0.25 nm centered at film position z based on their initial z coordinates at $t = 0$.

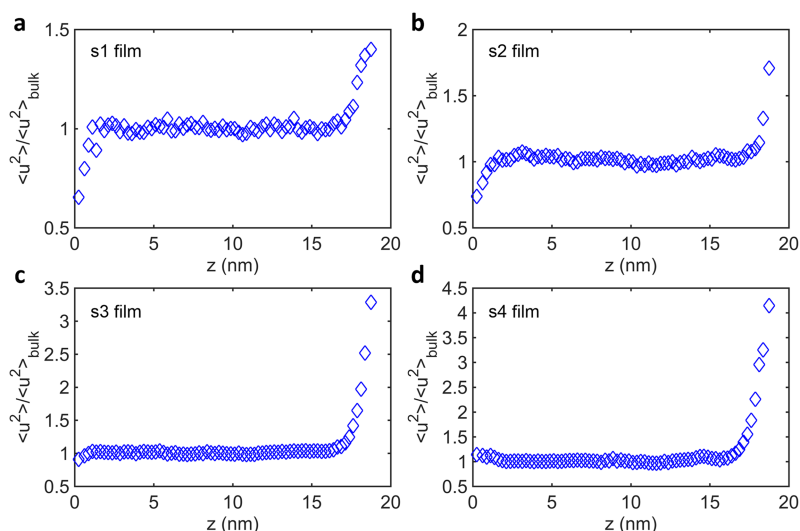


FIG. 8. Local Debye-Waller factor $\langle u^2 \rangle$ as a function of the film position z from the substrate-film interface to the free surface, normalized by their bulk value $\langle u^2 \rangle_{bulk}$ at temperature of their bulk T_g for different film systems: (a) s1, (b) s2, (c) s3, and (d) s4.

Fig. 8 shows the results of the local $\langle u^2 \rangle$ normalized by their respective values at bulk T_g for different film systems. Similar to the local T_g results, the local $\langle u^2 \rangle$ shows spatial variation as the position moves from the substrate-film interface towards the free surface, although the length scale of local $\langle u^2 \rangle$ variation is smaller than that of local T_g . Generally, the local $\langle u^2 \rangle$ is suppressed near the interface and enhanced near the free surface. However, as the side-group size increases (i.e., s1 to s4), the magnitude of local $\langle u^2 \rangle$ suppression near the substrate becomes less, while the magnitude of their enhancement near the free surfaces becomes greater. For film system s4 (i.e., the largest side-group size), there is in fact no decrease in local $\langle u^2 \rangle$ near the substrate. This is likely caused by the increased bulkiness of the polymer, which reduces the packing efficiency of the polymer near the substrate. With bulky side-groups, the packing hindrance near the attractive interface should give rise to less mobility restriction as induced by the substrate, which would lower the T_g enhancement induced by the substrate. The local mobility results corroborate our adhesion energy findings in Fig. 7, and provide a clear picture of how side-group size influences the substrate and free surface effects.

IV. CONCLUSIONS

The contribution of our work is two-fold. First, we demonstrate that side-group size plays an important role in governing the glass formation properties. As the side-group size increases, both T_g and fragility increase in the bulk state, which is consistent with theoretical predictions. Second, we show that there exists a correlation between the side-group size and confinement effects, which governs the strength of T_g -confinement in supported films. An increase in side-group size causes a stronger free-surface effect as manifested by the greater T_g reduction near the free surface. However, near the substrate, the enhancement of local T_g is less for the polymer with a larger side-group and a greater fragility, indicating a weaker confinement effect induced by the substrate. Through a DWF $\langle u^2 \rangle$ analysis, we find that the strength of the confinement effects on T_g is strongly correlated with local $\langle u^2 \rangle$. The suppression of the local $\langle u^2 \rangle$ near the substrate is less with greater side-group size, which suggests that the diminishing substrate effect for the bulkier side-group is due to the inefficient chain packing and lower adhesion near the attractive interface, leading to less mobility restriction and diminished enhancement in local T_g . Our findings help draw a molecular-level picture of T_g -confinement effects in supported thin films, and ascertain that polymer side-group size and fragility are important parameters that govern glass formation in both bulk and nanoconfined supported thin film states.

SUPPLEMENTARY MATERIAL

See [supplementary material](#) for the full CG potentials of the polymer models and an additional analysis of relaxation dynamics.

ACKNOWLEDGMENTS

W.X., J.S., D.D.H., and S.K. acknowledge support by the National Institute of Standards and Technology (NIST)

through the Center for Hierarchical Materials Design (CHiMaD) and from the Department of Civil and Environmental Engineering and Mechanical Engineering at Northwestern University. W.X. gratefully acknowledges the support from the NIST-CHiMaD Fellowship. A supercomputing grant from Quest HPC System at Northwestern University is acknowledged. We thank our collaborator Dr. Jack F. Douglas for fruitful discussions.

- ¹H. Ito, in *Microlithography Molecular Imprinting* (Springer, Heidelberg, 2005), Vol. 172, pp. 37–245.
- ²P. M. Ajayan, L. S. Schadler, and P. V. Braun, *Nanocomposite Science and Technology* (Wiley, New York, 2006).
- ³F. Truica-Marasescu and M. R. Wertheimer, *Plasma Processes Polym.* **5**(1), 44–57 (2008).
- ⁴J. L. Keddie, R. A. L. Jones, and R. A. Cory, *Europhys. Lett.* **27**(1), 59 (1994).
- ⁵C. J. Ellison and J. M. Torkelson, *Nat. Mater.* **2**(10), 695–700 (2003).
- ⁶J. A. Forrest, K. Dalnoki-Veress, J. R. Stevens, and J. R. Dutcher, *Phys. Rev. Lett.* **77**, 2002–2005 (1996).
- ⁷J. A. Forrest, K. Dalnoki-Veress, and J. R. Dutcher, *Phys. Rev. E* **56**(5), 5705–5716 (1997).
- ⁸C. B. Roth and J. R. Dutcher, *J. Electroanal. Chem.* **584**(1), 13–22 (2005).
- ⁹A. Bansal, H. Yang, C. Li, K. Cho, B. C. Benicewicz, S. K. Kumar, and L. S. Schadler, *Nat. Mater.* **4**(9), 693–698 (2005).
- ¹⁰J. A. Forrest and K. Dalnoki-Veress, *Adv. Colloid Interface Sci.* **94**, 167–196 (2001).
- ¹¹T. Lan and J. M. Torkelson, *Polymer* **55**(5), 1249–1258 (2014).
- ¹²C. M. Evans, H. Deng, W. F. Jager, and J. M. Torkelson, *Macromolecules* **46**(15), 6091–6103 (2013).
- ¹³J. Wang and G. B. McKenna, *Macromolecules* **46**(6), 2485–2495 (2013).
- ¹⁴D. S. Fryer, R. D. Peters, E. J. Kim, J. E. Tomaszewski, J. J. de Pablo, P. F. Nealey, C. C. White, and W. L. Wu, *Macromolecules* **34**(16), 5627–5634 (2001).
- ¹⁵R. D. Priestley, M. K. Mundra, N. J. Barnett, L. J. Broadbelt, and J. M. Torkelson, *Aust. J. Chem.* **60**(10), 765–771 (2007).
- ¹⁶R. P. White, C. C. Price, and J. E. Lipson, *Macromolecules* **48**(12), 4132–4141 (2015).
- ¹⁷Y. Grohens, M. Brogly, C. Labbe, M. O. David, and J. Schultz, *Langmuir* **14**(11), 2929–2932 (1998).
- ¹⁸J. L. Keddie, R. A. L. Jones, and R. A. Cory, *Faraday Discuss.* **98**, 219–230 (1994).
- ¹⁹C. B. Roth and J. M. Torkelson, *Macromolecules* **40**(9), 3328–3336 (2007).
- ²⁰P. Z. Hanakata, J. F. Douglas, and F. W. Starr, *Nat. Commun.* **5**, 4163 (2014).
- ²¹W. Xia, S. Mishra, and S. Keten, *Polymer* **54**(21), 5942–5951 (2013).
- ²²T. Lan and J. M. Torkelson, *Polymer* **64**, 183–192 (2015).
- ²³K. Kunal, C. G. Robertson, S. Pawlus, S. F. Hahn, and A. P. Sokolov, *Macromolecules* **41**(19), 7232–7238 (2008).
- ²⁴J. H. Mangalara and D. S. Simmons, *ACS Macro Lett.* **4**(10), 1134–1138 (2015).
- ²⁵W.-S. Xu and K. F. Freed, *Macromolecules* **47**(19), 6990–6997 (2014).
- ²⁶E. B. Stukalin, J. F. Douglas, and K. F. Freed, *J. Chem. Phys.* **131**(11), 114905 (2009).
- ²⁷S. Mirigian and K. S. Schweizer, *J. Chem. Phys.* **140**(19), 194506 (2014).
- ²⁸S. Mirigian and K. S. Schweizer, *J. Chem. Phys.* **140**(19), 194507 (2014).
- ²⁹T. Lan and J. M. Torkelson, *Macromolecules* **49**(4), 1331–1343 (2016).
- ³⁰S.-J. Xie, H.-J. Qian, and Z.-Y. Lu, *J. Chem. Phys.* **142**(7), 074902 (2015).
- ³¹J. M. Torres, C. Wang, E. B. Coughlin, J. P. Bishop, R. A. Register, R. A. Riggleman, C. M. Stafford, and B. D. Vogt, *Macromolecules* **44**(22), 9040–9045 (2011).
- ³²A. Shavit and R. A. Riggleman, *Macromolecules* **46**(12), 5044–5052 (2013).
- ³³P. Z. Hanakata, J. F. Douglas, and F. W. Starr, *J. Chem. Phys.* **137**(24), 244901 (2012).
- ³⁴B. A. Betancourt, P. Z. Hanakata, F. W. Starr, and J. F. Douglas, *Proc. Natl. Acad. Sci. U. S. A.* **112**(10), 2966–2971 (2015).
- ³⁵W. Xia and S. Keten, *Langmuir* **29**(41), 12730–12736 (2013).
- ³⁶D. D. Hsu, W. Xia, S. G. Arturo, and S. Keten, *J. Chem. Theory Comput.* **10**(6), 2514–2527 (2014).
- ³⁷F. Müller-Plathe, *ChemPhysChem* **3**(9), 754–769 (2002).

- ³⁸D. Reith, M. Putz, and F. Muller-Plathe, *J. Comput. Chem.* **24**(13), 1624–1636 (2003).
- ³⁹S. Plimpton, *J. Comput. Phys.* **117**(1), 1–19 (1995).
- ⁴⁰M. C. Payne, M. P. Teter, D. C. Allan, T. A. Arias, and J. D. Joannopoulos, *Rev. Mod. Phys.* **64**(4), 1045–1097 (1992).
- ⁴¹W. Xia, D. D. Hsu, and S. Keten, *Macromol. Rapid Commun.* **36**(15), 1422–1427 (2015).
- ⁴²M. D. Marvin, R. J. Lang, and D. S. Simmons, *Soft Matter* **10**(18), 3166–3170 (2014).
- ⁴³H. Vogel, *Phys Z* **22**, 645–646 (1921).
- ⁴⁴G. S. Fulcher, *J. Am. Ceram. Soc.* **8**(6), 339–355 (1925).
- ⁴⁵G. Tammann and W. Hesse, *Z. Anorg. Allg. Chem.* **156**(1), 245–257 (1926).
- ⁴⁶W. L. Merling, J. B. Mileski, J. F. Douglas, and D. S. Simmons, *Macromolecules* **49**(19), 7597–7604 (2016).
- ⁴⁷J. Dudowicz, K. F. Freed, and J. F. Douglas, in *Advances in Chemical Physics* (John Wiley & Sons, Inc., 2008), pp. 125–222.
- ⁴⁸R. A. Riddleman, J. F. Douglas, and J. J. de Pablo, *J. Chem. Phys.* **126**(23), 234903 (2007).
- ⁴⁹K. Jin and J. M. Torkelson, *Macromolecules* **49**(14), 5092–5103 (2016).
- ⁵⁰G. B. DeMaggio, W. E. Frieze, D. W. Gidley, M. Zhu, H. A. Hristov, and A. F. Yee, *Phys. Rev. Lett.* **78**(8), 1524–1527 (1997).
- ⁵¹W. Xia, D. D. Hsu, and S. Keten, *Macromolecules* **47**(15), 5286–5294 (2014).
- ⁵²C. Ye, C. G. Wiener, M. Tyagi, D. Uhrig, S. V. Orski, C. L. Soles, B. D. Vogt, and D. S. Simmons, *Macromolecules* **48**(3), 801–808 (2015).
- ⁵³C. L. Soles, J. F. Douglas, W. L. Wu, and R. M. Dimeo, *Phys. Rev. Lett.* **88**(3), 037401 (2002).
- ⁵⁴P. C. Chung, E. Glynnos, and P. F. Green, *Langmuir* **30**(50), 15200–15205 (2014).
- ⁵⁵F. W. Starr, S. Sastry, J. F. Douglas, and S. C. Glotzer, *Phys. Rev. Lett.* **89**(12), 125501 (2002).
- ⁵⁶R. Inoue, T. Kanaya, K. Nishida, I. Tsukushi, and K. Shibata, *Phys. Rev. Lett.* **95**(5), 056102 (2005).
- ⁵⁷R. W. Hall and P. G. Wolynes, *J. Chem. Phys.* **86**(5), 2943–2948 (1987).
- ⁵⁸W. Xia, J. K. Song, D. D. Hsu, and S. Keten, *Macromolecules* **49**(10), 3810–3817 (2016).
- ⁵⁹W. Xia and S. Keten, *Extreme Mech. Lett.* **4**, 89–95 (2015).